

# Multiple Domains of GlcNAc-1-phosphotransferase Mediate Recognition of Lysosomal Enzymes\*

Received for publication, January 7, 2016, and in revised form, January 28, 2016 Published, JBC Papers in Press, February 1, 2016, DOI 10.1074/jbc.M116.714568

Eline van Meel<sup>1,2</sup>, Wang-Sik Lee<sup>1</sup>, Lin Liu<sup>1</sup>, Yi Qian<sup>3</sup>, Balraj Doray, and Stuart Kornfeld<sup>4</sup>

From the Department of Internal Medicine, Washington University School of Medicine, St. Louis, Missouri 63110

The Golgi enzyme UDP-GlcNAc:lysosomal enzyme *N*-acetylglucosamine-1-phosphotransferase (GlcNAc-1-phosphotransferase), an  $\alpha_2\beta_2\gamma_2$  hexamer, mediates the initial step in the addition of the mannose 6-phosphate targeting signal on newly synthesized lysosomal enzymes. This tag serves to direct the lysosomal enzymes to lysosomes. A key property of GlcNAc-1-phosphotransferase is its unique ability to distinguish the 60 or so lysosomal enzymes from the numerous non-lysosomal glycoproteins with identical Asn-linked glycans. In this study, we demonstrate that the two Notch repeat modules and the DNA methyltransferase-associated protein interaction domain of the  $\alpha$  subunit are key components of this recognition process. Importantly, different combinations of these domains are involved in binding to individual lysosomal enzymes. This study also identifies the  $\gamma$ -binding site on the  $\alpha$  subunit and demonstrates that in the majority of instances the mannose 6-phosphate receptor homology domain of the  $\gamma$  subunit is required for optimal phosphorylation. These findings serve to explain how GlcNAc-1-phosphotransferase recognizes a large number of proteins that lack a common structural motif.

critical step in the generation of the Man-6-P tag is mediated by the Golgi enzyme UDP-GlcNAc:lysosomal enzyme *N*-acetylglucosamine-1-phosphotransferase (GlcNAc-1-phosphotransferase). This enzyme binds selectively to conformation-dependent protein determinants in the 60 or so lysosomal acid hydrolases and transfers GlcNAc-1-P from UDP-GlcNAc to mannose residues on high mannose-type *N*-linked glycans of the hydrolases (2). The GlcNAc is subsequently excised by a second Golgi enzyme (“uncovering enzyme”) to generate the high affinity Man-6-P ligand (3).

GlcNAc-1-phosphotransferase is an  $\alpha_2\beta_2\gamma_2$  hexamer that is encoded by two genes (4–7). The *GNPTAB* gene encodes the  $\alpha$  and  $\beta$  subunits, whereas the *GNPTG* gene encodes the  $\gamma$  subunit. Enzyme kinetic studies have indicated that the  $\alpha$  and  $\beta$  subunits specifically bind lysosomal acid hydrolases and mediate the catalytic function of the enzyme (8, 9). The  $\gamma$  subunit enhances the rate of GlcNAc-P transfer to a subset of the acid hydrolases without substantially altering the binding to these acceptors. Consistent with this, analysis of the level of mannose phosphorylation of the acid hydrolases in the brain of mice lacking the  $\gamma$  subunit, as estimated by the extent of binding to a cation-independent (CI)-MPR affinity resin, indicated that about one-third of the acid hydrolases were phosphorylated at close to wild-type (WT) levels, whereas another third were poorly phosphorylated with the final third showing intermediate levels of phosphorylation (9).

These studies leave unanswered the key question of how GlcNAc-1-phosphotransferase specifically recognizes lysosomal acid hydrolases. In looking for clues, we examined the domain structures of the  $\alpha$ ,  $\beta$ , and  $\gamma$  subunits of this transferase (10). The  $\alpha/\beta$  subunits contain three identifiable domains as follows: the Stealth domain, two Notch repeat modules, and a DNA methyltransferase-associated protein (DMAP) interaction domain. The Stealth domain resembles sequences within bacterial genes that encode sugar-phosphate transferases involved in cell wall polysaccharide synthesis and has been shown to mediate the catalytic function of GlcNAc-1-phosphotransferase (8, 10, 11). Importantly, the bacterial genes lack the Notch repeats and the DMAP interaction domain, which has been proposed to function as a protein-protein interaction domain (12). Because the bacterial enzymes transfer sugar-phosphates directly to polysaccharide acceptors without the involvement of protein recognition, we hypothesized that the mammalian transferase, in the course of protein evolution, acquired the Notch and DMAP interaction domains to function in the specific recognition of protein determinants on lysosomal acid hydrolases.

Correct targeting of newly synthesized acid hydrolases to lysosomes is essential for this organelle to maintain its function of degrading intracellular and endocytosed material. In higher eukaryotes, this process is mediated by the mannose 6-phosphate (Man-6-P)<sup>5</sup> recognition system whereby the newly synthesized acid hydrolases acquire Man-6-P residues in the Golgi that serve as high affinity ligands for binding to Man-6-P receptors (MPRs) in the *trans*-Golgi network and subsequent transport to the endo-lysosomal system (1). The initial and most

\* This work was supported by National Institutes of Health Grant CA-008759 and the Yash Gandhi Foundation. The authors declare that they have no conflicts of interest with the contents of this article. The content is solely the responsibility of the authors and does not necessarily represent the official views of the National Institutes of Health.

<sup>1</sup> These authors contributed equally to this work.

<sup>2</sup> Present address: Dept. of Medical Biochemistry, Leiden Institute of Chemistry, Leiden University, P. O. Box 9502, 2300 RA, Leiden, The Netherlands.

<sup>3</sup> Present address: Shanghai Institute for Advanced Immunochemical Studies, Shanghai Tech University, Bldg. 6, No. 99 Haik Rd., Pudong, Shanghai 201210, China.

<sup>4</sup> To whom correspondence should be addressed: Dept. of Internal Medicine, Hematology Division, Campus Box 8125, Washington University School of Medicine, 660 South Euclid Ave., St. Louis, MO 63110. Tel.: 314-362-8803; Fax: 314-362-8826; E-mail: skornfel@dom.wustl.edu.

<sup>5</sup> The abbreviations used are: Man-6-P, mannose 6-phosphate; CI, cation-independent; MPR, Man-6-P receptor; CathD, cathepsin D;  $\beta$ -Hex,  $\beta$ -hexosaminidase;  $\alpha$ MM,  $\alpha$ -methyl D-mannoside; MRH, Man-6-P receptor homology; PAPP, pregnancy-associated plasma protein; DMAP, DNA methyltransferase-associated protein.

## Function of GlcNAc-1-phosphotransferase Protein Domains

Support for this hypothesis has come from studies of the consequences of missense mutations in Notch 1 and the DMAP interaction domain found in patients with the autosomal recessive lysosomal storage disorders mucopolisidosis II and III (10, 13). These mutations were shown to impair lysosomal enzyme phosphorylation without altering the catalytic activity of the transferase toward the simple sugar  $\alpha$ -methyl D-mannoside ( $\alpha$ MM). This is consistent with a role for these domains in binding to lysosomal enzymes.

The  $\gamma$  subunit contains two recognizable domains as follows: a Man-6-P receptor homology (MRH) domain (14, 15), and a DMAP interaction domain (this study). The MRH domain contains residues critical for mannose binding, but it lacks those needed for phosphate binding (15). Although it has not been shown to bind high mannose oligosaccharides, similar MRH domains in other proteins do so (16, 17). The function of the MRH and DMAP interaction domains of the  $\gamma$  subunit in lysosomal acid hydrolase phosphorylation has not been examined to date.

To gain a better understanding of the role of the domains of the  $\alpha$ ,  $\beta$ , and  $\gamma$  subunits of GlcNAc-1-phosphotransferase in lysosomal enzyme recognition, we used the CRISPR/Cas9 genome-editing system to inactivate the *GNPTAB* and *GNPTG* genes in HeLa cells and then determined the ability of various mutants of these genes to restore phosphorylation of a panel of lysosomal enzymes and proteins.

Our findings establish that the two Notch repeats along with the DMAP interaction domain of the  $\alpha$  subunit of GlcNAc-1-phosphotransferase mediate the specific recognition of lysosomal acid hydrolases. Furthermore, we present evidence that the requirement for the individual protein interacting domains to achieve phosphorylation varies among the acid hydrolase substrates. We also show that the  $\gamma$  subunit binds to the spacer region between Notch 2 and the DMAP interaction domain, and we document a variable requirement for the MRH domain and the DMAP interaction domain of the  $\gamma$  subunit. Together, these findings provide new insight into how lysosomal acid hydrolases are selectively recognized by GlcNAc-1-phosphotransferase.

### Experimental Procedures

**Cell Lines**—*GNPTAB*<sup>-/-</sup> and *GNPTG*<sup>-/-</sup> HeLa cells were generated by CRISPR nuclease-induced targeted double strand break at the Genome Engineering Center at Washington University School of Medicine (St. Louis, MO). HeLa cells were obtained from ATCC (parental line). Exon 3 of *GNPTAB* was targeted with guide RNA 5'-GTAAACAACGTCATCG-GCA-3', whereas Exon 2 of *GNPTG* was targeted with guide RNA 5'-TTCGCTGCACCTGCCGCGC-3' (Fig. 1). Sequencing determined that all three alleles of *GNPTAB* were disrupted with one allele having a 17-bp deletion, c.216\_232del, whereas the other two alleles had a 1-bp deletion c.221delC. In the case of *GNPTG*, all three alleles had an insertion, c.61insT, c.61insA, and c.61insG (see Fig. 1). All cell lines were maintained in DMEM (Mediatech, Inc.) containing 0.11 g/liter sodium pyruvate and 4.5 g/liter glucose, supplemented with 10% (v/v) FBS (Atlanta Biologicals), 100,000 units/liter penicil-

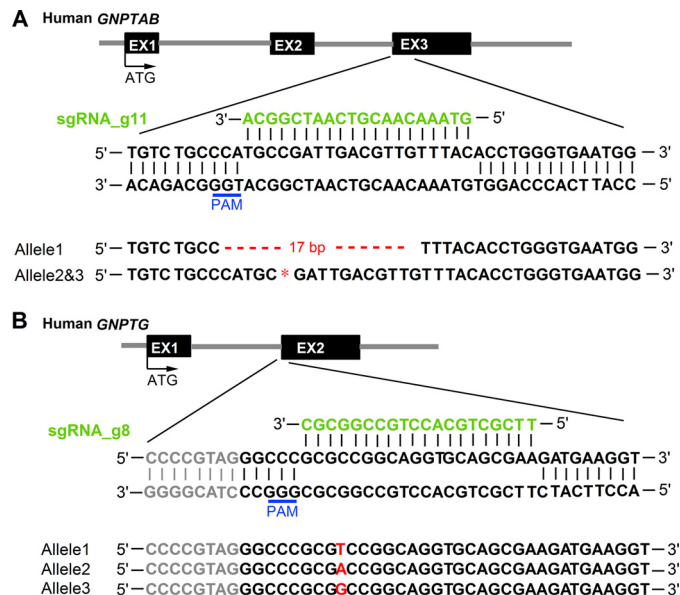


**FIGURE 1. Generation of *GNPTAB*<sup>-/-</sup> and *GNPTG*<sup>-/-</sup> HeLa cell lines using CRISPR/Cas9 genome editing.** A and B, schematic of the base pairing between a guide RNA (sgRNA\_g11 for *GNPTAB* and sgRNA\_g8 for *GNPTG*) and the targeting loci of the two genes. The sequences of the mutated alleles are shown. All the insertions and deletions cause frameshift mutations and early termination of translation.

lin, 100 mg/liter streptomycin (Life Technologies, Inc.), and 2 mM L-glutamine (Mediatech).

**DNA Constructs**—Human  $\gamma$ DMAP (amino acids 173–267) cDNA was PCR-amplified from human *GNPTG*-FLAG cDNA in pcDNA3.1(+) (10) and cloned into pGEX-6P-1 (GE Healthcare) using general molecular cloning techniques. Human *GNPTG*-FLAG in pcDNA3.1(+) was modified by QuikChange site-directed mutagenesis to generate the various mutant  $\gamma$  constructs. The full cDNA sequences were confirmed by DNA sequencing. Human *GNPTAB*-V5/His in pcDNA6 has been described (10). The various  $\alpha/\beta$  deletion constructs were made by a two-step overlap-extension PCR process wherein the native cDNA restriction fragment encoding the Notch 1-DMAP (amino acids 438–819) sequence was swapped with a similar PCR-generated restriction fragment encoding the specific deletion. The two Notch 1 repeat-containing construct was generated by a three-step overlap-extension PCR process. All of the sequences were confirmed to be correct by DNA sequencing. In preliminary experiments, we found that deletion of residues 431–819 gave rise to a mutant protein that was well expressed and localized to the Golgi but had no catalytic activity toward  $\alpha$ MM, in agreement with De Pace *et al.* (18). By contrast, the  $\Delta$ 438–819 mutant had full catalytic activity (see Fig. 3).

To generate the  $\alpha/\beta$  and  $\gamma$  bicistronic construct, a 1.5-kb gBlocks gene fragment was synthesized (IDT Inc.) that encoded the internal ribosomal entry site sequence from the pTandem vector (EMD Millipore), followed by the human  $\gamma$  cDNA sequence with the hemagglutinin (HA) tag nucleotide sequence in-frame at the 3' end.

The NPC2 cDNA construct was generously provided by Daniel Ory (Washington University School of Medicine, St. Louis, MO). Sandra Hofmann (University of Texas Southwest-

ern Medical Center, Dallas) kindly provided the cDNA construct for PPT1.

**Immunofluorescence Microscopy**—To visualize lysosomes, parental, *GNPTAB*<sup>-/-</sup> and *GNPTG*<sup>-/-</sup> HeLa cells were fixed and stained as described (10), using mouse anti-human LAMP-1 (H4A3-s) monoclonal antibody (Developmental Studies Hybridoma Bank, Iowa City, IA).

To visualize the subcellular localization of the  $\alpha/\beta$  and  $\gamma$  subunits, the various constructs were transfected into parental or *GNPTAB*<sup>-/-</sup> HeLa cells using Lipofectamine 3000 (Life Technologies, Inc.) according to the manufacturer's protocol. Co-transfection of  $\alpha/\beta$  and  $\gamma$  subunit cDNAs was performed using an 8:1 ratio, respectively. 24 h post-transfection, the cells were fixed, and the  $\alpha/\beta$  subunits were detected with affinity-purified rabbit anti- $\alpha$  antibody with the exception of the  $\Delta$ N1-DMAP and the  $\Delta$ DMAP deletions, which were detected with mouse anti-V5 monoclonal antibody (Life Technologies, Inc.). The reason for this is that the rabbit anti- $\alpha$  antibody is directed against an epitope within the DMAP domain. This necessitated the use of two different Golgi markers, GM130 and GOLPH4, which were detected with mouse anti-GM130 monoclonal antibody (BD Biosciences) and rabbit anti-GOLPH4 polyclonal antibody (Abcam), respectively. The  $\gamma$  subunit was detected with either rabbit anti- $\gamma$  antiserum that was kindly provided by Thomas Braulke (University Medical Center Hamburg-Eppendorf, Hamburg, Germany) or with mouse anti-FLAG M2 monoclonal antibody (Sigma).

The processed cells were mounted in ProLong<sup>®</sup> Gold anti-fade mounting medium (Life Technologies, Inc.), and the images were acquired with either a Zeiss LSM510 or an LSM880 confocal microscope (Carl Zeiss Inc.). Images were analyzed by ImageJ software (Fiji).

**Binding of  $\alpha/\beta$  to  $\gamma$** —To determine binding of WT or mutant  $\alpha/\beta$  to WT or mutant  $\gamma$ , HEK 293 cells were either transfected with the co-expression bicistronic vector or co-transfected with the individual  $\alpha/\beta$  and  $\gamma$  plasmids. Twenty four hours post-transfection, cells were lysed in ice-cold buffer A (50 mM NaH<sub>2</sub>PO<sub>4</sub>, 300 mM NaCl, 0.5% Tween 20, 10 mM imidazole, and protease inhibitors) and clarified by centrifugation at 15,000  $\times$  g. The supernatant was added to Ni-NTA beads (Life Technologies, Inc.) and tumbled for 2 h at 4 °C. Beads were washed three times with ice-cold buffer B (buffer A with 20 mM imidazole and no protease inhibitors), boiled in SDS sample buffer, and the bound proteins resolved by SDS-PAGE, transferred to nitrocellulose, and detected by Western blotting.

**CI-MPR Affinity Chromatography and Enzyme Assays**—Soluble bovine CI-MPR was purified from FBS and covalently conjugated to cyanogen bromide-activated Sepharose 4B (Sigma) at 1 mg/ml as described (19). Two days post-transfection, HeLa cells in a 6-well plate were collected and lysed with 250  $\mu$ l of cell lysis buffer (25 mM Tris-Cl, pH 7.2, 150 mM NaCl, 1% Triton X-100) containing protease inhibitors. 20  $\mu$ l of the CI-MPR-Sepharose beads was washed twice with lysis buffer, and mixed with 200  $\mu$ l of cell lysate. The mixture was incubated for 1 h at 4 °C with tumbling and then centrifuged at 2,400  $\times$  g for 2 min to pellet the beads, which were washed twice with lysis buffer containing 5 mM glucose 6-phosphate. Finally, the beads were resuspended in lysis buffer containing 10 mM Man-6-P to elute

the bound proteins. Lysosomal enzyme assays were performed on the eluates as described previously (10). The enzyme activity was normalized to the total protein concentration of the different cell extracts.

**GST Pulldown Experiments**—The protocol for purification of CathD from porcine spleen is detailed elsewhere (20, 21).  $\alpha$ -GalA was a generous gift from Amicus Therapeutics (Cranbury, NJ), whereas  $\alpha$ -iduronidase was kindly provided by William Canfield (Genzyme, Boston, MA). GST and GST fusions were expressed in and purified from *Escherichia coli* BL21 (RIL) cells (Agilent Technologies), and pull-down assays were performed with the purified lysosomal enzymes exactly as described (13).

**Western Blotting**—Proteins resolved by SDS-PAGE under reducing or non-reducing conditions were transferred to nitrocellulose membrane and detected with antibodies as indicated in the figure legends.

**[2-<sup>3</sup>H]Mannose Labeling Experiments**—Labeling experiments were performed with parental, *GNPTAB*<sup>-/-</sup>, and *GNPTG*<sup>-/-</sup> HeLa cells as follows. 48 h post-transfection, cells in 60-mm tissue culture plates were incubated with 50–150  $\mu$ Ci of [2-<sup>3</sup>H]mannose (PerkinElmer Life Sciences) for 2 h, followed by the addition of complete medium containing 5 mM glucose, 5 mM mannose, and 10 mM NH<sub>4</sub>Cl to stop mannose uptake and induce secretion. The cells were incubated for an additional 3 h before the media were collected. In several experiments, cell extracts were prepared and subjected to Western blotting for  $\beta$  subunit content to confirm that the constructs were being expressed at comparable levels.

**Immunoprecipitation and Oligosaccharide Analysis**—Acid hydrolases secreted into the media were immunoprecipitated, and oligosaccharides were isolated and analyzed essentially as described in detail previously (22). For the CathD-myc,  $\alpha$ -Man-myc, NPC2-myc, and  $\beta$ -Man-HA experiments, 20  $\mu$ l of anti-Myc monoclonal antibody (Santa Cruz Biotechnology) or 5  $\mu$ l of anti-HA monoclonal antibody (Sigma) was pre-bound to 100  $\mu$ l of protein G-agarose-PLUS beads (Santa Cruz Biotechnology) prior to immunoprecipitation of labeled lysosomal hydrolases from the media. In the case of  $\alpha$ -Gal and PPT1, the secreted enzymes were immunoprecipitated with protein G-agarose-PLUS beads pre-bound to anti- $\alpha$ -Gal antibody (Amicus Therapeutics) and rProtein A-agarose beads (Repligen) pre-bound to anti-PPT1 antibody (kindly provided by Sandra Hofmann, University of Texas Southwestern Medical Center, Dallas, TX), respectively. Immunoprecipitated material was treated with endoglycosidase H (New England Biolabs) and filtered with Ultracel-10K (EMD Millipore). The filtrate containing neutral and phosphorylated high mannose glycans was treated with mild acid to remove any *N*-acetylglucosamine residues still attached to the phosphate moieties and applied to a QAE-column matrix to separate the oligosaccharides bearing zero, one, or two Man-6-P residues. The retentate containing Endo H-resistant complex oligosaccharides was treated with Pronase (Roche Diagnostics) and fractionated on concanavalin A-Sepharose 4B (GE Healthcare). The [2-<sup>3</sup>H]mannose content of each fraction was determined, and the percent phosphorylation was calculated as described (22). In all cases, values obtained in the mock transfection were subtracted.

## Function of GlcNAc-1-phosphotransferase Protein Domains

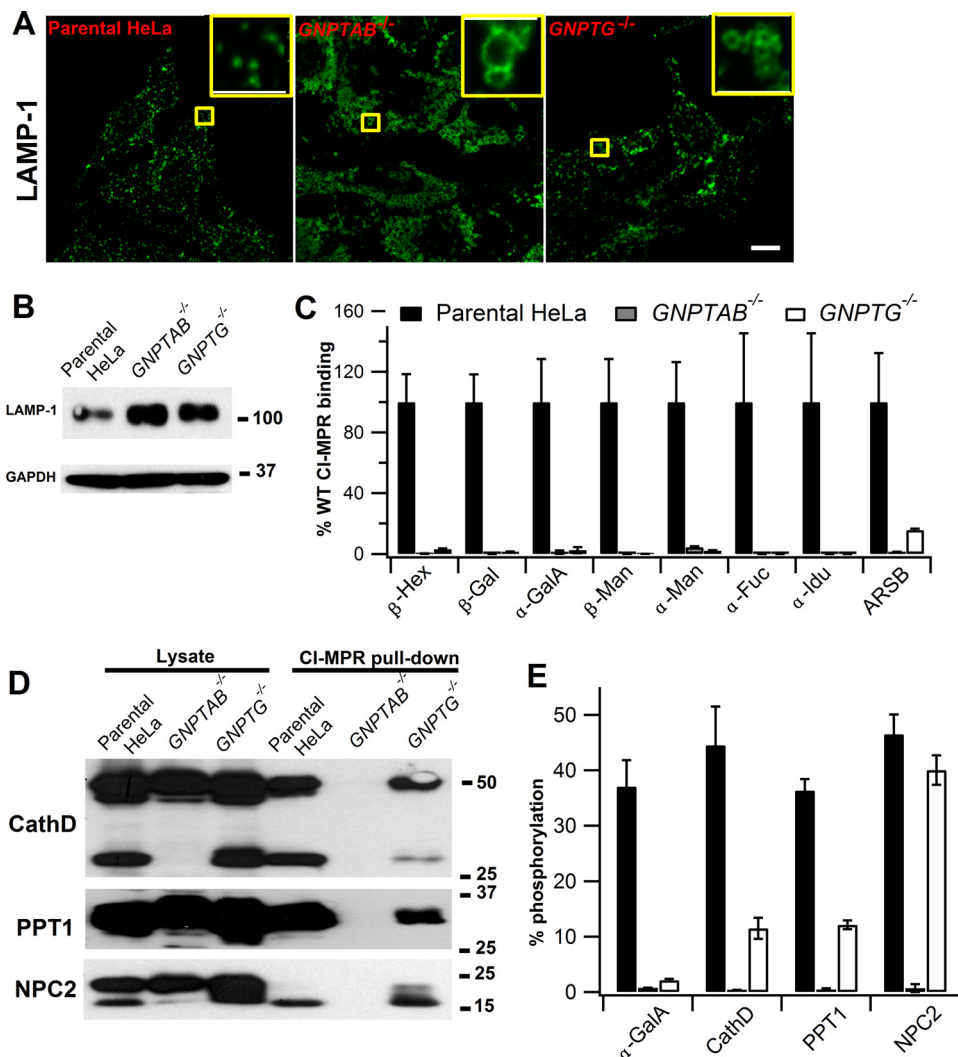


FIGURE 2. *GNPTAB*<sup>-/-</sup> and *GNPTG*<sup>-/-</sup> HeLa cells have enlarged lysosomes and are deficient in phosphorylated lysosomal proteins. *A*, confocal immunofluorescence images of parental,  $\alpha/\beta$ -deficient, and  $\gamma$ -deficient HeLa cells, stained for the late endosomal/lysosomal marker LAMP-1 (green). Scale bar, 10  $\mu$ m. *B*, immunoblot of cell lysates (20  $\mu$ g per lane) from parental,  $\alpha/\beta$ -deficient, and  $\gamma$ -deficient HeLa cells probed for LAMP-1. *C*, lysates of the three cell lines were incubated with CI-MPR affinity beads, and the binding of the various lysosomal proteins was determined by enzyme assays. Mean values obtained with the parental HeLa cells are set to 100%  $\pm$  S.D. ( $n = 3-5$ ). *D*, lysates of the three cell lines were incubated with CI-MPR affinity beads, and the binding of the three lysosomal proteins was determined by Western blots. *E*, WT and mutant cells transfected with plasmids encoding the four lysosomal proteins were labeled with [<sup>2-3</sup>H]mannose, followed by immunoprecipitation of the proteins secreted into the media and determination of the percent *N*-glycans containing Man-6-P. The percentage oligosaccharide phosphorylation  $\pm$  S.D. for each enzyme in the three different cell lines is shown ( $n = 2-5$ ).

## Results

*GNPTAB*<sup>-/-</sup> and *GNPTG*<sup>-/-</sup> HeLa Cells Are Differentially Impaired in Lysosomal Enzyme Phosphorylation—To analyze the function of the various domains of the subunits of GlcNAc-1-phosphotransferase, we needed cell lines that lacked either the  $\alpha/\beta$  or  $\gamma$  subunits while maintaining good growth and being readily transfectable. To achieve this goal, the CRISPR/Cas9 genome-editing system was used to generate *GNPTAB*<sup>-/-</sup> and *GNPTG*<sup>-/-</sup> HeLa cells. Confocal immunofluorescence microscopy of these cells using the lysosomal/late endosomal marker LAMP-1 revealed a striking enlargement of lysosomes in both lines compared with the parental HeLa cells, with the abnormality being greatest in the *GNPTAB*<sup>-/-</sup> cells (Fig. 2*A*). Both knock-out cell lines had a dramatic increase in LAMP-1 content, as documented by Western blots for this membrane protein (Fig. 2*B*). These findings are indicative of

major lysosomal dysfunction in the mutant cells. Despite this, the cells grew well and were readily transfectable.

Whole cell extracts of the *GNPTAB*<sup>-/-</sup> and *GNPTG*<sup>-/-</sup> cells had low but detectable levels of a panel of lysosomal acid hydrolases based on enzymatic assays. To determine whether the residual hydrolases observed in the *GNPTAB*<sup>-/-</sup> and *GNPTG*<sup>-/-</sup> cells contained any Man-6-P residues, we measured their binding to beads containing immobilized CI-MPR, which exhibits high affinity binding to phosphorylated lysosomal proteins (23). Seven of the eight hydrolases assayed in the *GNPTAB*<sup>-/-</sup> lysates exhibited less than 1% of the binding observed with the WT extract, whereas  $\alpha$ -mannosidase ( $\alpha$ -Man) had 4% of WT binding (Fig. 2*C*). This indicates that most of the residual activities measured in the whole cell extract from *GNPTAB*<sup>-/-</sup> cells are in fact non-phosphorylated lysosomal enzymes that are in the process of traversing the secre-

tory pathway. Binding of these hydrolases in the *GNPTG*<sup>-/-</sup> lysates to immobilized CI-MPR was also greatly reduced (Fig. 2C), but in three instances it was substantially increased over that observed with the same enzymes from *GNPTAB*<sup>-/-</sup> cells as follows: arylsulfatase B, 16 ± 0.4% versus 1.2 ± 0.1%; β-hexosaminidase (β-Hex), 3.4 ± 1.5% versus 0.3 ± 0.2%; and β-galactosidase (β-Gal), 1.3 ± 0.5% versus 0.1 ± 0.1%. In addition to these acid hydrolases, the eluates of the CI-MPR affinity beads were also analyzed for their content of cathepsin D (CathD), Niemann-Pick disease, type C2 (NPC2), and palmitoyl-protein thioesterase (PPT1) by Western blotting (Fig. 2D). Whereas all three proteins were found in the eluate of the WT cell lysate, none were detected in the eluate of the *GNPTAB*<sup>-/-</sup> cell lysate. By contrast, two of these proteins (CathD and PPT1) were present at substantial albeit reduced levels in the eluate of the *GNPTG*<sup>-/-</sup> cell lysate, whereas NPC2 was recovered at close to the WT level.

We next turned to the use of [2-<sup>3</sup>H]mannose labeling to obtain quantitative determinations of the degree of Man-6-P formation on the various lysosomal proteins. In these experiments, cells were transfected with cDNA constructs encoding the lysosomal proteins, and 48 h later, the cells were labeled for 2 h with [2-<sup>3</sup>H]mannose and then chased for 3 h in the presence of NH<sub>4</sub>Cl to stimulate lysosomal protein secretion. The protein of interest was then immunoprecipitated from the media and the percent of the N-linked high mannose glycans that contained Man-6-P residues determined as described under "Experimental Procedures." This procedure avoids any loss of Man-6-P that may occur if the phosphorylated proteins were to reach the lysosome. As shown in Fig. 2E, in all instances the lysosomal proteins expressed in the *GNPTAB*<sup>-/-</sup> cells contained less than 1% Man-6-P-containing glycans whereas the same proteins expressed in WT cells were well phosphorylated (36–47% Man-6-P-containing glycans). Similar to the findings with the CI-MPR binding assays, α-galactosidase A (α-GalA) was poorly phosphorylated in the *GNPTG*<sup>-/-</sup> cells, whereas CathD and PPT1 were phosphorylated 26 ± 4% and 33 ± 2% as well as occurred in WT cells, whereas NPC2 was phosphorylated 86 ± 6% of the WT level. These findings confirm that the requirement for the γ subunit of GlcNAc-1-phosphotransferase to achieve optimal phosphorylation varies greatly among the lysosomal proteins.

**Deletion of the α Subunit Notch 1-DMAP Interaction Domain (Residues 438–819) Abolishes Acid Hydrolase Phosphorylation**—To test the hypothesis that the α subunit Notch repeat modules and the DMAP interaction domain function as protein recognition elements, a construct with deletion of residues 438–819 (ΔN1-DMAP) of the α/β precursor was prepared. This construct lacked both Notch repeats and the DMAP interaction domain along with the intervening spacer regions (Fig. 3A). The ΔN1-DMAP construct was well expressed and, in fact, gave rise to substantially more mature α/β than the construct encoding the WT α/β precursor (Fig. 3B). As the cleavage of the α/β precursor is mediated by the site 1 protease in the Golgi (24), the finding of increased levels of the β subunit indicates that the mutant protein is efficiently delivered to the Golgi. This was confirmed by showing that the deletion mutant co-localized with the Golgi marker, GOLPH4, using confocal immuno-

fluorescence microscopy (Fig. 3C). Furthermore, the mutant protein exhibited strong activity toward the simple sugar αMM, consistent with an increased level of cleaved β subunit (Fig. 3D). This establishes that the catalytic function of this mutant was intact. Importantly, the lysosomal acid hydrolases of *GNPTAB*<sup>-/-</sup> cells transfected with the deletion mutant failed to acquire any detectable Man-6-P, in contrast to transfection with the construct encoding WT α/β precursor (Fig. 3E). Thus, in the absence of the Notch repeats and the DMAP interaction domain, this catalytically active, Golgi-localized GlcNAc-1-phosphotransferase lost its ability to phosphorylate lysosomal acid hydrolases. This finding establishes that these domains are required for the selective recognition of acid hydrolase substrates.

**γ Subunit Binds to the Spacer Region (Residues 535–694) of the α Subunit**—Because the function of the ΔN1-DMAP construct would be impaired if the binding of the γ subunit was lost, it became necessary to identify the binding site on the α/β precursor for the γ subunit and determine whether or not the ΔN1-DMAP construct harbors this site. In the initial experiment, the WT α/β precursor and the ΔN1-DMAP construct were co-expressed with the γ subunit in *GNPTAB*<sup>-/-</sup> cells, followed by confocal immunofluorescence microscopy to determine the subcellular distribution of the various subunits. Cells transfected with the γ subunit alone served as a control. As shown in Fig. 3F, the γ subunit co-localized with the WT α/β subunits in the Golgi but was undetectable in the Golgi of cells transfected with the ΔN1-DMAP construct or with γ alone. These findings indicate that the γ subunit localizes to the Golgi via binding to the α/β subunits and that this interaction is lost in the ΔN1-DMAP construct, implicating this region of the α subunit as the γ-binding site.

To localize the γ subunit-binding site more precisely, a series of constructs with deletion of either Notch 1, Notch 2, the spacer region (S2) between Notch 2 and the DMAP interaction domain, and the DMAP interaction domain itself were prepared (Fig. 4A). These constructs were expressed in HeLa cells where they localized to the Golgi and exhibited good catalytic activity toward αMM (Fig. 4, B–D). The various constructs were then tested for their ability to bind the γ subunit. For these assays, HEK 293 cells were either transfected with a bicistronic vector that encoded the various α/β constructs containing a C-terminal V5-His tag along with the γ subunit with a C-terminal HA tag (Fig. 5A) or co-transfected with individual plasmids encoding α/β or γ (Fig. 5B). Twenty four hours post-transfection, the cells were lysed and the α/β subunits affinity-purified on Ni-NTA beads. The bound subunits were eluted, subjected to SDS-PAGE, and analyzed for the content of β and γ subunits by Western blotting. As shown in Fig. 5, A and B, the γ subunit co-purified with the WT, ΔN1, ΔN2, and ΔDMAP α/β constructs but was not detectable in the ΔS2, ΔN1-DMAP, and ΔN2-DMAP mutants. This establishes that the γ subunit binds to the 535–694-amino acid spacer region of the α subunit. Because the ΔN1, ΔN2, and ΔDMAP interaction domain constructs retain γ subunit binding, any impairment of these mutant proteins in lysosomal enzyme phosphorylation cannot be attributed to the lack of the γ subunit.

## Function of GlcNAc-1-phosphotransferase Protein Domains

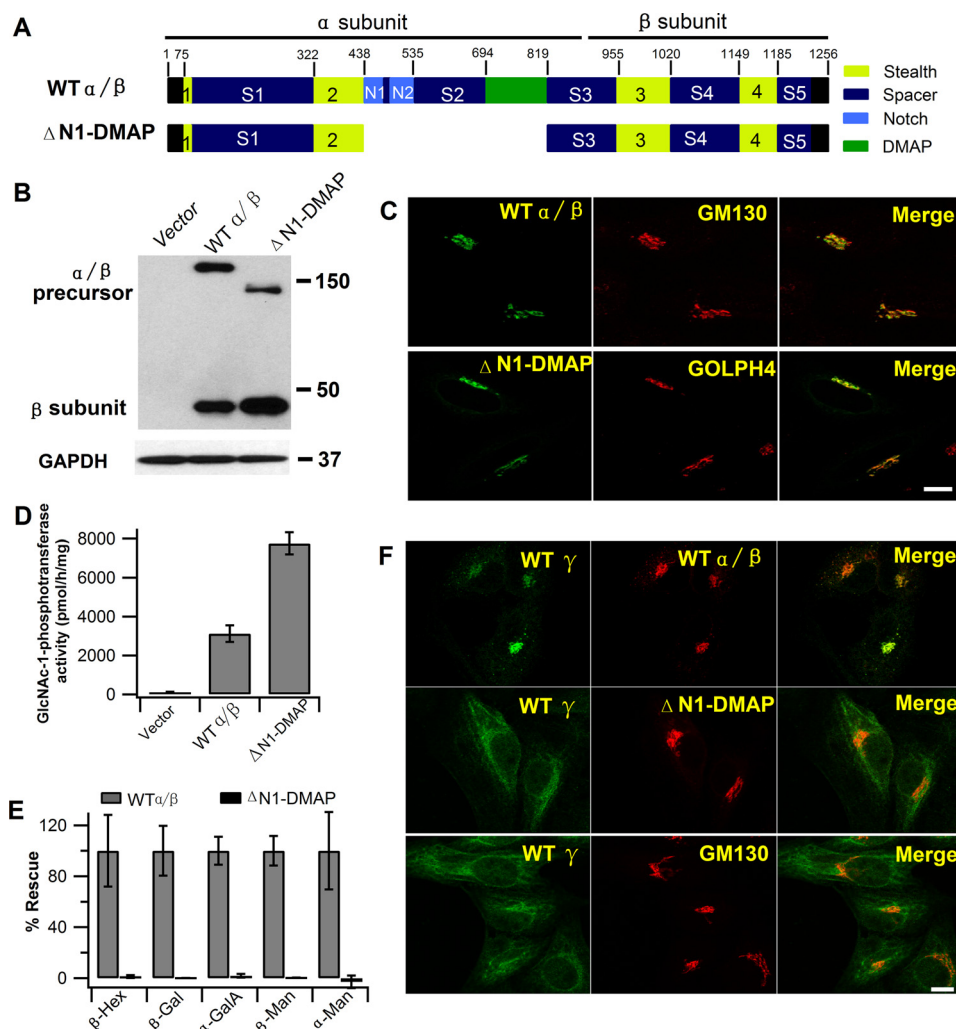


**FIGURE 3. The  $\Delta$ N1-DMAP mutant has catalytic activity but is unable to phosphorylate lysosomal enzymes.** *A*, schematic of GlcNAc-1-phosphotransferase  $\alpha/\beta$  subunit modular arrangement and deletion of the Notch 1 through DMAP interaction domain (residues 438–819). *B*, immunoblot analysis of WT  $\alpha/\beta$  versus the  $\Delta$ N1-DMAP deletion mutant expressed in *GNPTAB*<sup>-/-</sup> HeLa cells probed with anti-V5 antibody. *C*, confocal immunofluorescence images of parental HeLa cells transfected with WT  $\alpha/\beta$  or the  $\Delta$ N1-DMAP mutant and co-localized with the Golgi markers GM130 or GOLPH4, respectively (see “Experimental Procedures”). *D*, phosphotransferase activity toward the simple sugar  $\alpha$ MM, using extracts of *GNPTAB*<sup>-/-</sup> cells transfected with vector, WT  $\alpha/\beta$ , or  $\Delta$ N1-DMAP mutant plasmids. *E*, transfection of *GNPTAB*<sup>-/-</sup> HeLa cells with WT  $\alpha/\beta$  but not the  $\Delta$ N1-DMAP mutant restores lysosomal enzyme phosphorylation as determined by binding to CI-MPR affinity beads. Mean values obtained with cells transfected with WT  $\alpha/\beta$  are set to 100%  $\pm$  S.D. *F*, confocal immunofluorescence images of *GNPTAB*<sup>-/-</sup> cells co-expressing  $\gamma$  with WT  $\alpha/\beta$  (top) or with the  $\Delta$ N1-DMAP mutant (bottom). Scale bars, 10  $\mu$ m.

**Effect of the  $\alpha/\beta$  Deletion Mutants on Restoration of Lysosomal Enzyme Phosphorylation**—The ability of the  $\alpha/\beta$  deletion mutants to restore phosphorylation of five endogenous acid glycosidases in *GNPTAB*<sup>-/-</sup> cells, as determined by the CI-MPR affinity binding assay, is shown in Fig. 6A with the values plotted as percent of rescue obtained with the WT construct. Deletion of Notch 2 strongly inhibited phosphorylation of all the glycosidases, whereas deletion of Notch 1 was less detrimental, with levels of phosphorylation ranging from 100% of WT ( $\alpha$ - and  $\beta$ -Man) down to 60% of WT ( $\beta$ -Hex). The effect of deleting the DMAP interaction domain was also variable, ranging from a 10% decrease in phosphorylation relative to WT ( $\beta$ -Hex) to a 64% decrease in  $\alpha$ -Man phosphorylation. Deletion of the S2 domain, which results in the loss of binding of the  $\gamma$  subunit, strongly inhibited phosphorylation of all the glycosidases. This was expected as these five enzymes are dependent on the  $\gamma$  subunit for phosphorylation (Fig. 2C).

Importantly, increasing the level of expression of the various constructs did not alter the extent of correction of phosphorylation. In all instances the level of expression was at least 6-fold greater than the endogenous activity in parental HeLa cells.

We next investigated the ability of the various  $\alpha/\beta$  deletion mutants to phosphorylate a panel of lysosomal proteins using the [<sup>3</sup>H]mannose-labeling procedure to quantitate the degree of phosphorylation. As shown in Fig. 6B, the consequences of deleting Notch 1, Notch 2, or the DMAP interaction domain on the generation of the Man-6-P residues on  $\alpha$ -GalA and  $\alpha$ - and  $\beta$ -Man as measured by this technique are mostly in agreement with the results obtained with the CI-MPR affinity resin binding assay. Thus, deletion of Notch 2 strongly inhibited phosphorylation of the three acid glycosidases, whereas loss of Notch 1 substantially lowered phosphorylation of  $\alpha$ -GalA, while having a smaller inhibitory effect on the other two glyco-

## Function of GlcNAc-1-phosphotransferase Protein Domains

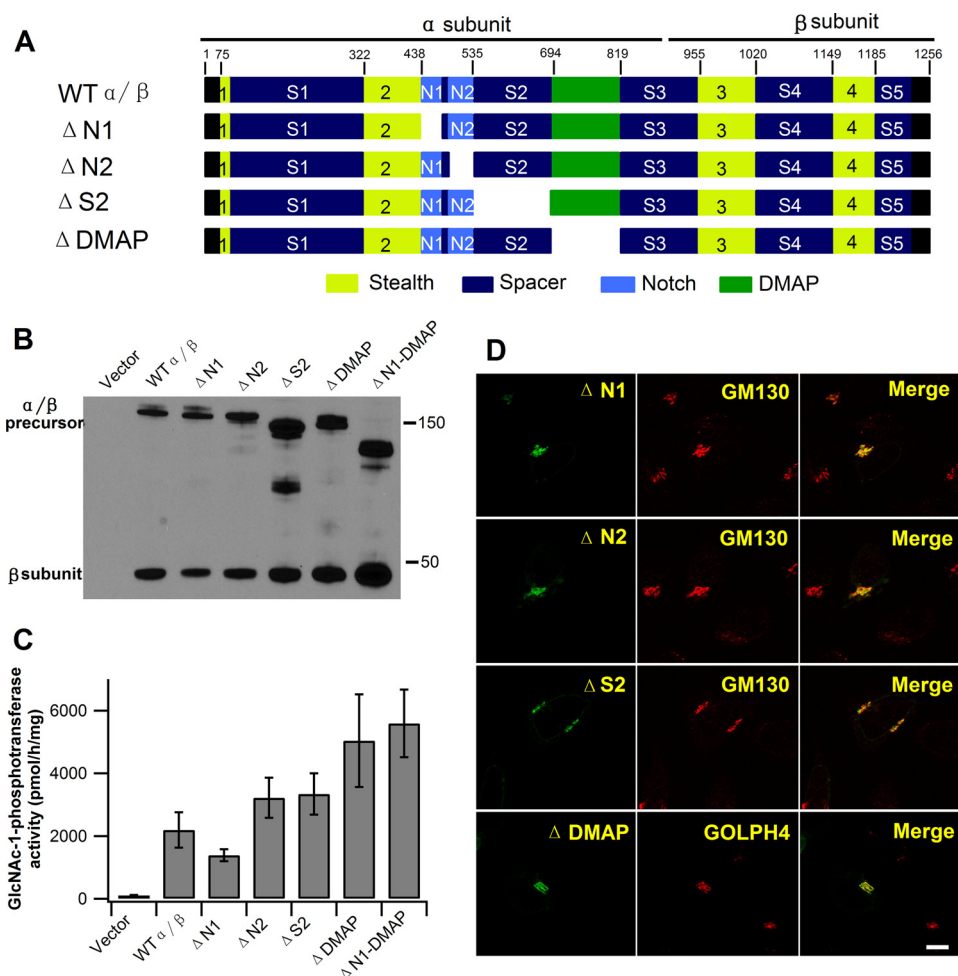


**FIGURE 4. Expression of deletion mutants of  $\alpha/\beta$ .** *A*, schematic of the various  $\alpha/\beta$  deletion constructs expressed in HEK 293 cells. *B*, Western blot of WT  $\alpha/\beta$  and mutants expressed in *GNPTAB*<sup>-/-</sup> HeLa cells. 20  $\mu$ g of each cell extract was loaded, and the  $\alpha/\beta$  precursor and  $\beta$  subunits were detected with an anti-V5 antibody. *C*, catalytic activity of WT  $\alpha/\beta$  and the mutants toward  $\alpha$ MM using equal amounts of whole cell extracts. The vector-only transfected *GNPTAB*<sup>-/-</sup> HeLa cell extract served as a control. *D*, confocal immunofluorescence microscopy of HeLa cells transfected with plasmids encoding the various  $\alpha/\beta$  deletion mutants. Cells were fixed 24 h post-transfection and probed with anti- $\alpha$  antibody ( $\Delta$ N1,  $\Delta$ N2, and  $\Delta$ S2), or with the anti-V5 antibody ( $\Delta$ DMAP). The Golgi markers, GM130 and GOLPH4, were detected with anti-GM130 and anti-GOLPH4 antibodies, respectively. Scale bar, 10  $\mu$ m.

sidases. The only significant discrepancy was observed with  $\alpha$ -Man where deletion of the DMAP interaction domain had a lesser effect on phosphorylation as measured by this assay. Also shown are the results with CathD, PPT1, and NPC2. The findings with NPC2 are of particular interest because the phosphorylation of this protein is mostly independent of the  $\gamma$  subunit. In this case, deletion of Notch 2 (58% versus 38% decrease in phosphorylation, respectively), whereas deletion of the DMAP interaction domain had no impact on phosphorylation. The finding that the  $\Delta$ N1-DMAP mutant phosphorylated NPC2 very poorly indicates that the two Notch modules are the critical domains in the phosphorylation of NPC2. The results were similar with PPT1 except in this case loss of Notch 2 was more detrimental than loss of Notch 1 (56% versus 30% decrease in phosphorylation, respectively). The phosphorylation of CathD, however, was completely lost in the absence of Notch 2 and 60% inhibited when Notch 1 was deleted.

Taken together, these findings show that the Notch 1 and 2 repeat modules and the DMAP interaction domain of the  $\alpha$  subunit all contribute to the generation of Man-6-P-residues

in lysosomal enzymes. However, their relative impact varies with each lysosomal enzyme. In addition, the  $\gamma$  subunit is critical for phosphorylation of a subset of the lysosomal proteins.

*Notch 1 Repeat Module Cannot Substitute for the Notch 2 Repeat Module*—One explanation for why deletion of the Notch 2 module impairs phosphorylation of most of the hydro-lases more than deletion of Notch 1 is that it mediates a function that cannot be carried out by Notch 1. Alternatively, it may be located in a more critical site of the transferase. To address this issue, a construct was prepared in which the Notch 2 module was replaced by the Notch 1 module (Fig. 7A). This approach preserved the overall spacing of the domains of the transferase. This construct was well expressed, localized to the Golgi, bound  $\gamma$ , and exhibited good catalytic activity toward  $\alpha$ MM (Fig. 7, B–E). However, it functioned only slightly better than the  $\Delta$ N2 construct in restoring the phosphorylation of endogenous acid glycosidases in the *GNPTAB*<sup>-/-</sup> cells (Fig. 7F). This finding clearly shows that Notch 1 is unable to functionally substitute for Notch 2 in GlcNAc-1-phosphotransferase.

## Function of GlcNAc-1-phosphotransferase Protein Domains

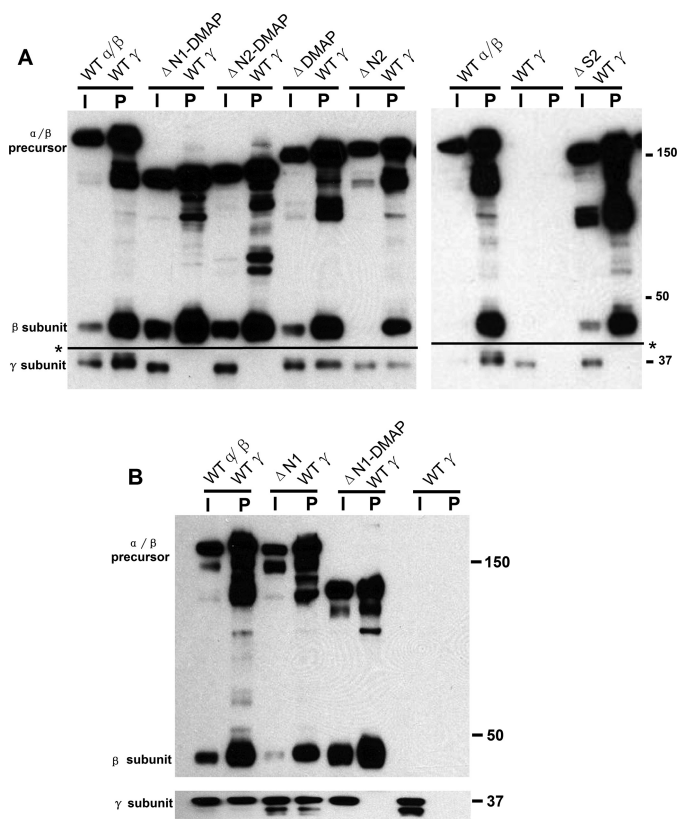


**FIGURE 5. The  $\gamma$  subunit binds to amino acids 535–694 of the  $\alpha$  subunit.** A and B, lysates of HEK 293 cells expressing WT  $\alpha/\beta$  or the deletion mutants along with WT  $\gamma$  were incubated with Ni-NTA affinity beads to pull down the various forms of the  $\alpha/\beta$  subunits.  $\gamma$  only served as a control. The bound material was assayed for the content of  $\alpha/\beta$  and  $\gamma$  subunits by SDS-PAGE and Western blotting using anti-V5 antibody to detect  $\alpha/\beta$  and anti-HA antibody (A) or anti-FLAG antibody (B) to detect  $\gamma$ . I, 3% of input; P, 25% of pellet fraction. \*, line denotes position where the nitrocellulose membrane was cut to allow for probing of the  $\alpha/\beta$  and  $\gamma$  subunits with different antibodies. Even long exposures of the blot failed to show detectable binding of  $\gamma$  to the  $\Delta N1$ -DMAP,  $\Delta N2$ -DMAP, and  $\Delta S2$  mutants of  $\alpha/\beta$  (data not shown).

**Rescue of Acid Hydrolase Phosphorylation in *GNPTG*<sup>-/-</sup> Cells by WT and Mutant  $\gamma$  Subunits**—The  $\gamma$  subunit contains the following two recognizable domains that are candidates for participating in lysosomal enzyme binding and phosphorylation: the MRH domain and the DMAP interaction domain. Although previously not recognized as such, blast analysis revealed that the  $\gamma$ DMAP interaction domain shares similarities with the DMAP interaction domain of the  $\alpha$  subunit (Fig. 8A) and shows significant conservation in the N-terminal half among various species (Fig. 8B). Similar to the previously reported findings with a GST fusion protein containing the DMAP interaction domain of the  $\alpha$  subunit (13), a GST fusion protein containing the DMAP interaction domain of the  $\gamma$  subunit pulled down several lysosomal hydrolases, but not the non-lysosomal protein tissue factor pathway inhibitor (Fig. 8C). The affinity of the GST- $\gamma$ DMAP was similar to that of GST- $\alpha$ DMAP based on the pattern of release of the bound glycosidases in the washing steps (Fig. 8D). In both cases, the amount of glycosidase activity released in the washes was much greater than that of the control GST. This supports the notion that the  $\gamma$  subunit may contribute to the binding of lysosomal acid hydrolases. Unfortunately, despite numerous attempts using

alanine scanning and deletion mutagenesis, we were unable to generate a  $\gamma$  subunit with a mutant DMAP interaction domain that had lost the ability to bind to acid hydrolases but retained proper folding in the endoplasmic reticulum and localization in the Golgi. This prevented us from directly analyzing the role of the  $\gamma$ DMAP interaction domain in the overall function of the  $\gamma$  subunit.

The MRH domain was inactivated by making an R134K/E153Q double mutation (Fig. 9A), as equivalent mutations in the MRH domain of the CI-MPR had been shown to abolish mannose binding without altering folding (15, 25). Preliminary experiments showed that the  $\gamma$  mutant was well expressed, interacted with the  $\alpha/\beta$  subunits in the Ni-NTA pulldown assay, and localized to the Golgi in a process that required co-expression of  $\alpha/\beta$  (Fig. 9, B and C). This indicates that the MRH mutations do not impair association with the  $\alpha/\beta$  precursor, exit from the endoplasmic reticulum, or localization in the Golgi.

The effect of the MRH mutations on the ability of the  $\gamma$  subunit to restore endogenous acid glycosidase phosphorylation in *GNPTG*<sup>-/-</sup> cells as determined by CI-MPR affinity resin binding is shown in Fig. 9D. These enzymes are highly dependent on the  $\gamma$  subunit for phosphorylation (Fig. 2C). In all cases, transfection of the WT  $\gamma$  subunit cDNA substantially restored phosphorylation. By contrast, the MRH mutant exhibited poor phosphorylation of these acid glycosidases, especially  $\alpha$ - and  $\beta$ -Man,  $\alpha$ -L-fucosidase ( $\alpha$ -Fuc), and  $\alpha$ -L-iduronidase ( $\alpha$ -Idu) (93–98% inhibition), while having somewhat better activity toward  $\beta$ -Hex,  $\beta$ -Gal, and  $\alpha$ -GalA (65–73% inhibition). A similar result was obtained with  $\alpha$ -GalA when the level of Man-6-P synthesis was determined by the [<sup>3</sup>H]mannose labeling procedure (Fig. 9E).

It is also apparent from Fig. 9E that the  $\gamma$  subunit enhancement of phosphorylation of CathD and PPT1 over the vector only control is largely dependent on an intact MRH domain. In the case of NPC2, the presence of the  $\gamma$  subunit had only a very small stimulatory effect on phosphorylation, but this effect also appeared to be MRH-dependent. Together, these findings demonstrate that the MRH domain of the  $\gamma$  subunit participates in the phosphorylation of acid hydrolases, although its role varies depending on the particular hydrolase in question.

## Discussion

Although the components of the Man-6-P targeting system have been known for many years, the critical issue of how GlcNAc-1-phosphotransferase selectively recognizes lysosomal acid hydrolases has remained a mystery. Enzyme kinetic studies using recombinant  $\alpha/\beta/\gamma$  and  $\alpha/\beta$  GlcNAc-1-phosphotransferase have indicated that the  $\alpha/\beta$  subunits mediate the binding to the conformation-dependent protein domain on the lysosomal enzymes as well as the catalytic function, whereas the  $\gamma$  subunit enhances the rate of GlcNAc-P transfer to a subset of the acceptors (9). Although informative, these studies did not address the role of the various domains of the transferase in these functions. Some insight into this question has come from the analysis of missense mutations in the *GNPTAB* gene present in patients with mucopolipidosis II and III



## Function of GlcNAc-1-phosphotransferase Protein Domains

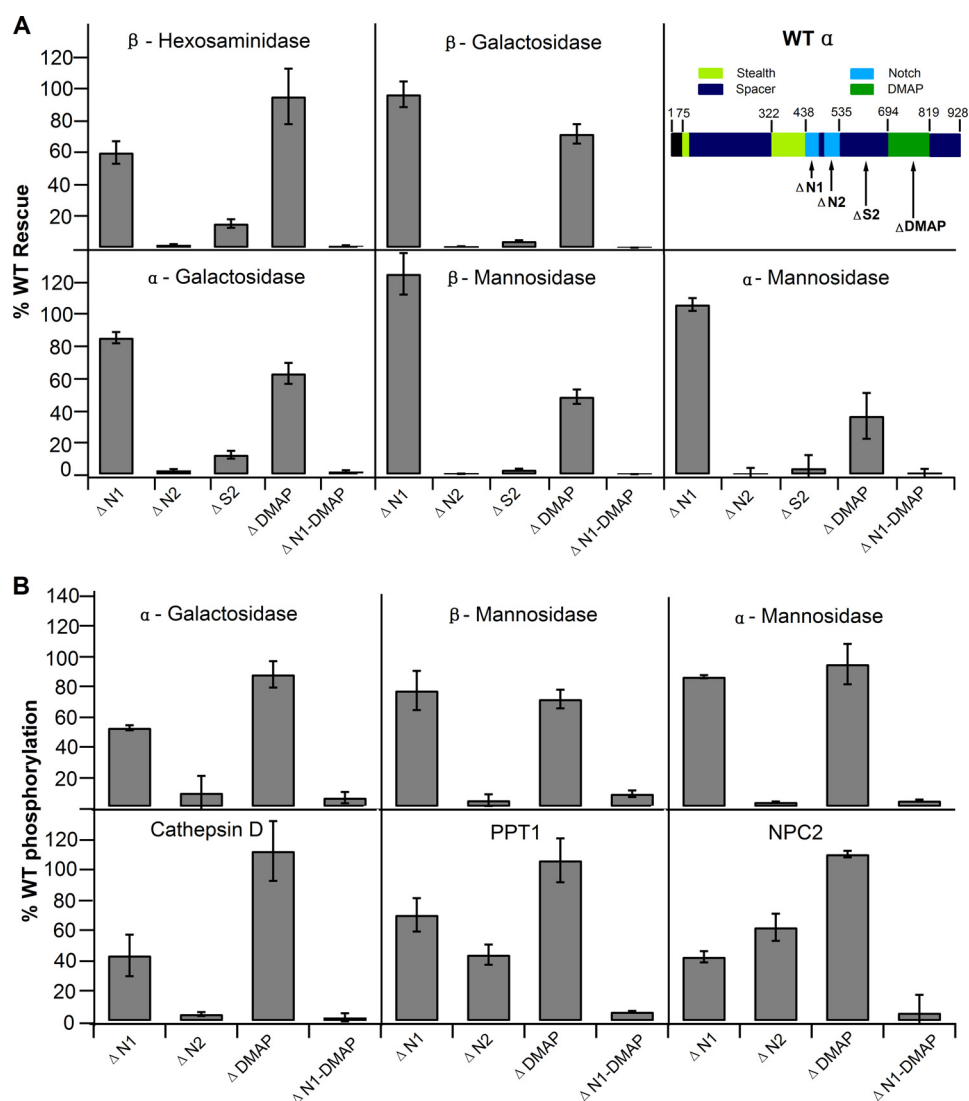


**FIGURE 6. Effect of the  $\alpha/\beta$  domain deletions on lysosomal enzyme phosphorylation.** *A*, lysates of  $GNPTAB^{-/-}$  HeLa cells transfected with WT or deletion mutants of  $\alpha/\beta$  were incubated with Cl-MPR affinity beads, and the bound material was assayed for the content of the various acid glycosidases. Mean values obtained with cells transfected with the various mutants are compared with WT  $\alpha/\beta$ , which is set to 100% ( $n = 3-5$ ). *B*,  $GNPTAB^{-/-}$  cells were co-transfected with the various forms of  $\alpha/\beta$  along with the indicated lysosomal protein encoding plasmids. Following [ $2\text{-}^3\text{H}$ ]mannose labeling, the degree of *N*-glycan phosphorylation of the lysosomal proteins was determined. Values obtained with the various mutants are compared with WT  $\alpha/\beta$ , which is set to 100% ( $n = 2-3$ ).

(10, 13). These studies implicated the Notch 1 repeat module and the DMAP interaction domain of the  $\alpha$  subunit in lysosomal acid hydrolase recognition. However, the limited number of patient mutations prevented analysis of some domains of the  $\alpha/\beta$  subunits as well as the  $\gamma$  subunit.

Two key advances in this study allowed us to overcome the limitations of the previous studies. The first was the use of CRISPR/Cas9 genome editing to generate readily transfectable HeLa cells in which the *GNPTAB* or the *GNPTG* gene had been inactivated. The second was the finding that single or multiple domains located in the middle of the *GNPTAB* gene could be deleted without impairing the catalytic function or Golgi localization of the gene product. In fact, deletion of Notch 1 through DMAP (residues 438–819) of the  $\alpha$  subunit gives rise to an  $\alpha/\beta$  precursor that exited the endoplasmic reticulum more efficiently than the WT species, localized properly to the Golgi, and retained full catalytic activity toward the simple sugar

$\alpha\text{MM}$ . This allowed for the interrogation of the function of these domains within this region.

The critical finding is that the Notch 1-DMAP deletion mutant failed to phosphorylate lysosomal enzymes demonstrating the essential role for this region of the  $\alpha$  subunit in GlcNAc-1-phosphotransferase function. Within this region we found that the Notch 1 and 2 repeat modules along with the DMAP interaction domain participate to varying degrees in the phosphorylation of individual lysosomal proteins. Thus, in the case of the glycosidases  $\beta\text{-Hex}$ ,  $\alpha\text{-GalA}$ ,  $\beta\text{-Gal}$ , and  $\alpha\text{-}$  and  $\beta\text{-Man}$ , the loss of Notch 2 inhibited phosphorylation much more than the loss of Notch 1 or the DMAP interaction domain. However, deletion of the DMAP interaction domain resulted in substantial inhibition of  $\beta\text{-Man}$  phosphorylation, whereas deletion of Notch 1 had no effect. The opposite was true in the case of  $\beta\text{-Hex}$ . The situation was different with NPC2 and PPT1 where loss of Notch 1 or Notch 2 resulted in similar impair-

## Function of GlcNAc-1-phosphotransferase Protein Domains

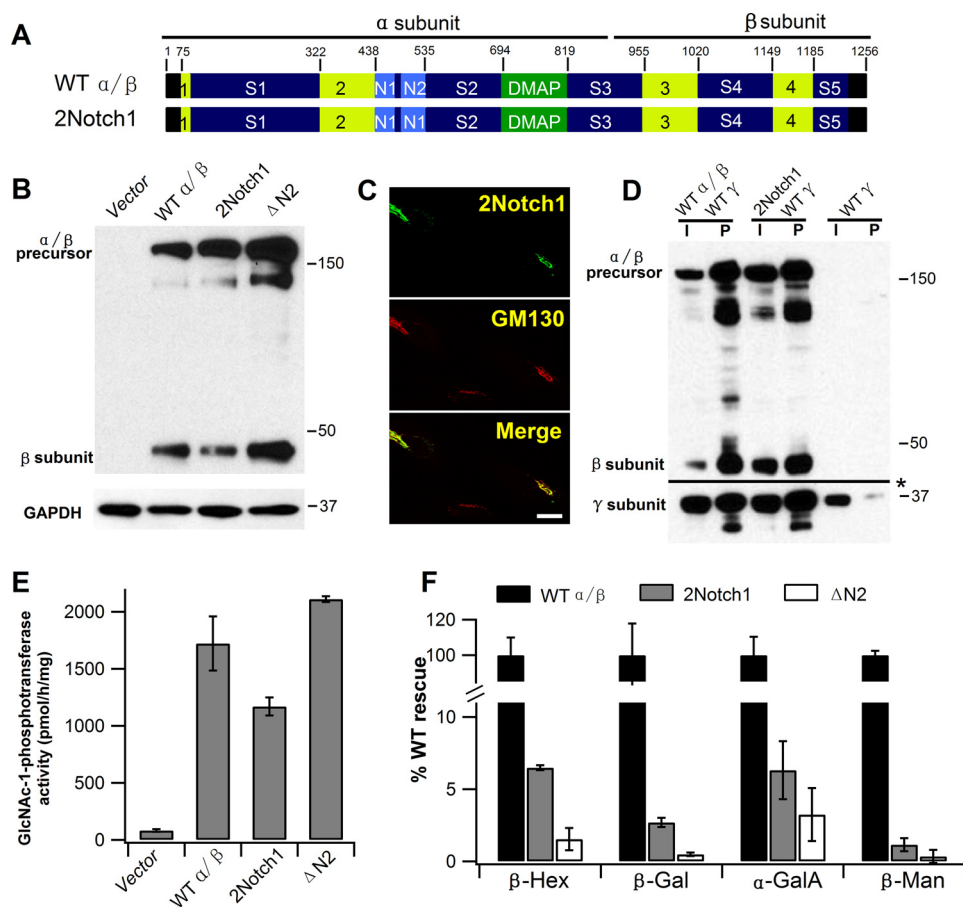


**FIGURE 7. Effect of substituting the Notch 2 repeat module with Notch 1.** *A*, schematic showing  $\alpha/\beta$  construct with two Notch 1 modules. *B*, Western blot of  $GNPTAB^{-/-}$  cells transfected with either WT  $\alpha/\beta$ , the 2Notch1 mutant, or the  $\Delta N2$  mutant. 20  $\mu\text{g}$  of each cell lysate was loaded. *C*, confocal immunofluorescence images of  $GNPTAB^{-/-}$  cells expressing the 2Notch1 mutant. Cells were fixed 24 h post-transfection and probed with anti- $\alpha$  antibody (2 Notch 1) and anti-GM130 antibody for the Golgi marker GM130. Scale bar, 10  $\mu\text{m}$ . *D*, lysates of HEK 293 cells expressing WT  $\alpha/\beta$  or the 2Notch1 mutant along with WT  $\gamma$  were incubated with Ni-NTA affinity beads to pull down the various forms of the  $\alpha/\beta$  subunits.  $\gamma$  only served as a control. The bound material was assayed for the content of  $\alpha/\beta$  and  $\gamma$  subunits by SDS-PAGE and Western blotting using anti-V5 antibody to detect  $\alpha/\beta$  and anti-FLAG antibody to detect  $\gamma$ . I, 3% of input; P, 25% of pellet fraction. *E*, phosphotransferase activity toward the simple sugar  $\alpha\text{MM}$ , using extracts of  $GNPTAB^{-/-}$  cells transfected with either vector, WT  $\alpha/\beta$ , the 2Notch1 mutant, or the  $\Delta N2$  mutant.  $n = 3$ . *F*,  $GNPTAB^{-/-}$  HeLa cells transfected with either WT  $\alpha/\beta$ , the 2Notch1 mutant, or the  $\Delta N2$  mutant were assayed for activity of the indicated enzymes as determined by binding to Cl-MPR affinity beads. Mean values obtained with the two mutants are compared with WT  $\alpha/\beta$ , which is set to 100%  $\pm$  S.D. ( $n = 3$ ). \*, line denotes position where the nitrocellulose membrane was cut to allow for probing of the  $\alpha/\beta$  and  $\gamma$  subunits with different antibodies.

ments of phosphorylation, whereas loss of the DMAP interaction domain had no effect on phosphorylation. Taken together, these data reveal a variable requirement for the Notch repeat modules and the  $\alpha\text{DMAP}$  interaction domain among this set of lysosomal proteins, although in most instances the Notch 2 module was dominant.

The inability of Notch 1 to restore acid hydrolase phosphorylation when inserted into the Notch 2 location points to a special role for Notch 2 in GlcNAc-1-phosphotransferase function. In this regard, it is notable that although the two Notch repeat modules have an identical number of residues and the same spacing of the three disulfide bonds, they only share 50% identity in amino acid sequence. Furthermore, the sequences of Notch 1 and Notch 2 are highly conserved among species, consistent with each module having a distinct role in the function of the transferase. At this point, the role of the Notch repeat modules in the selective phosphorylation of lysosomal acid hydrolases is unclear. One possibility that we are currently pursuing is that they directly engage the conformation-dependent binding site of the acid hydrolases. This would be consistent

with the role of the Notch repeat modules in other proteins. In the Notch receptors, the three tandemly repeated Notch modules function to prevent proteolytic cleavage of the receptor until binding of a physiologic ligand occurs (26). This autoinhibition is achieved by the Notch repeat modules forming numerous interdomain contacts that allow these modules to wrap around the juxtamembrane heterodimerization domain of the receptor and mask the protease cleavage site. Aside from the Notch receptors, the only other proteins reported to contain Notch repeat modules are the metalloproteinase pregnancy-associated plasma protein-A (PAPP-A) and its homologue PAPP-A2 (27, 28). These proteases act on a limited number of substrates, with PAPP-A cleaving only IGF-binding proteins 4 and 5, whereas PAPP-A2 only cleaves IGFBP-5. Importantly, the three Notch repeat modules of PAPP-A have been shown to mediate the proteolytic specificity of this enzyme toward IGFBP-4 (27). If the two Notch repeat modules of the  $\alpha$ -subunit of GlcNAc-1-phosphotransferase prove to directly interact with multiple lysosomal acid hydrolases, it will expand the role of these domains.

## Function of GlcNAc-1-phosphotransferase Protein Domains

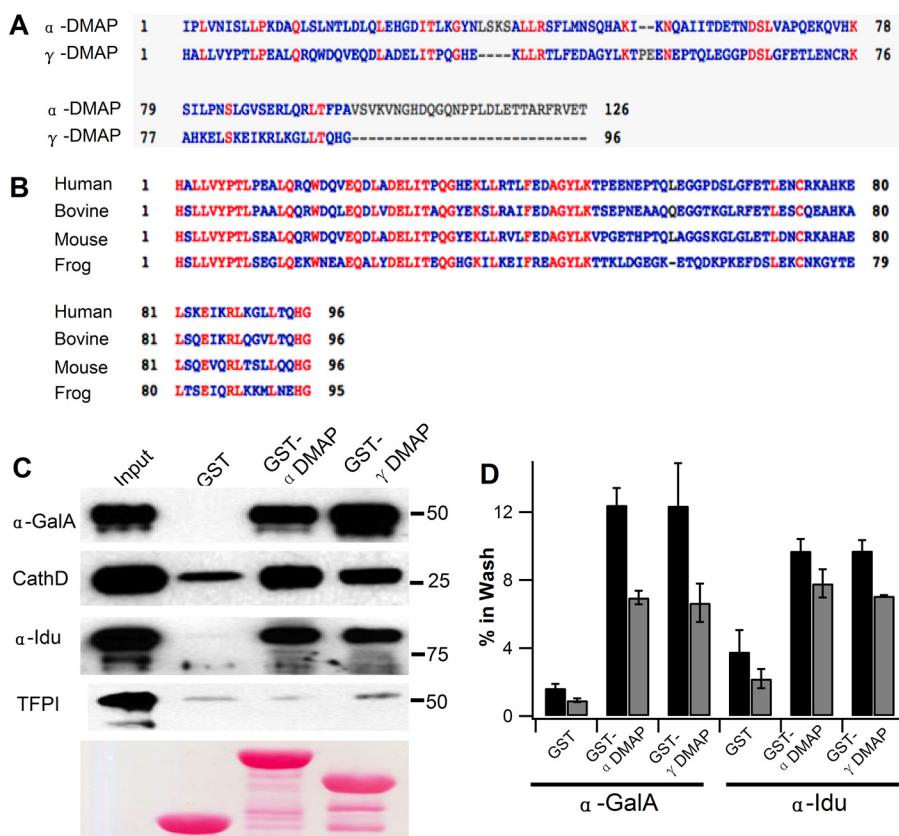


**FIGURE 8. The  $\gamma$ DMAP interaction domain binds lysosomal enzymes.** *A*, human  $\alpha/\beta$  and  $\gamma$ DMAP interaction domains are aligned with identical amino acid residues shown in red. *B*, alignment of the DMAP interaction domains of  $\gamma$  from several species shows a high degree of conservation in the N-terminal half of the domain. Because of the variation of 5 amino acid residues, only bovine  $\gamma$  shows up as a DMAP interaction domain in an NCBI Blast search. *C*, pull-down assays were performed with GST fusions to  $\alpha/\beta$  and  $\gamma$ DMAP interaction domains using the purified lysosomal enzymes indicated, along with tissue factor pathway inhibitor (TFPI), a non-lysosomal secreted glycoprotein. 0.2% of the input and 20% of the pellet fraction was loaded. *D*, release of bound enzyme activity was measured following wash steps 1 and 2 to determine loss of bound material as a result of the wash steps ( $n = 2$ ).

With regard to the role of the  $\alpha$ DMAP interaction domain, it should be noted that we previously reported that the K732N and L785W missense mutations in this domain were defective in phosphorylating purified porcine CathD *in vitro*, and the K732N mutant was impaired in correcting the phenotypic abnormalities observed in a zebrafish model of ML II (13). Therefore, it was surprising that the  $\Delta$ DMAP mutant phosphorylated CathD quite well in the current transfection studies while exhibiting defective phosphorylation of several other lysosomal hydrolases. The reason for this discrepancy is not clear at this time.

Another key observation is that the binding site for the  $\gamma$  subunit resides in the spacer region (amino acids 535–694) located between the Notch 2 and DMAP interaction domains. As the  $\gamma$  subunit facilitates phosphorylation of most of the lysosomal hydrolases, it appears that all of the elements involved in the selective phosphorylation of lysosomal proteins are localized to one region of the transferase. It should be noted that while this manuscript was in preparation, De Pace *et al.* (18), using a different approach, reported that the  $\gamma$  subunit binds to the same spacer region of the  $\alpha$  subunit. These data do not exclude additional roles for the spacer region between amino acids 535–694.

Consistent with our previous findings with *GNPTG*<sup>-/-</sup> mice (9), we observed a variable impact on the phosphorylation of the lysosomal proteins of *GNPTG*<sup>-/-</sup> HeLa cells. This ranged

from a modest 15% decrease in phosphorylation of NPC2 to almost a complete loss of phosphorylation of a number of the acid glycosidases. To gain insight into how the  $\gamma$  subunit functions in the phosphorylation process, we analyzed the role of the MRH domain of this subunit. Although the presence of the MRH domain of the  $\gamma$  subunit was initially recognized in 2001 (14), this is the first study to directly address its role in lysosomal protein phosphorylation. Our findings clearly show that mutating MRH residues required for mannose binding inhibits the ability of  $\gamma$  to facilitate the phosphorylation of those lysosomal acid hydrolases that are dependent on this subunit. These results indicate that binding of the MRH domain to the high mannose oligosaccharides of the acid hydrolases is central to the function of the  $\gamma$  subunit.

How might this be important? A clue comes from the analysis of the phosphorylation of various acid hydrolases. A number of studies have found that among acid hydrolases with multiple *N*-linked glycans, only a subset of the glycans are phosphorylated (29–33). This can be explained if some of the glycans have unfavorable locations on the surface of the hydrolase relative to the site of the protein recognition domains where GlcNAc-1-phosphotransferase docks. Presumably only glycans within a certain range of the docking site will be able to engage the catalytic elements of the transferase (34, 35). We have previously speculated that binding of the  $\gamma$ MRH domain to selected high mannose glycans with unfavorable locations may

## Function of GlcNAc-1-phosphotransferase Protein Domains

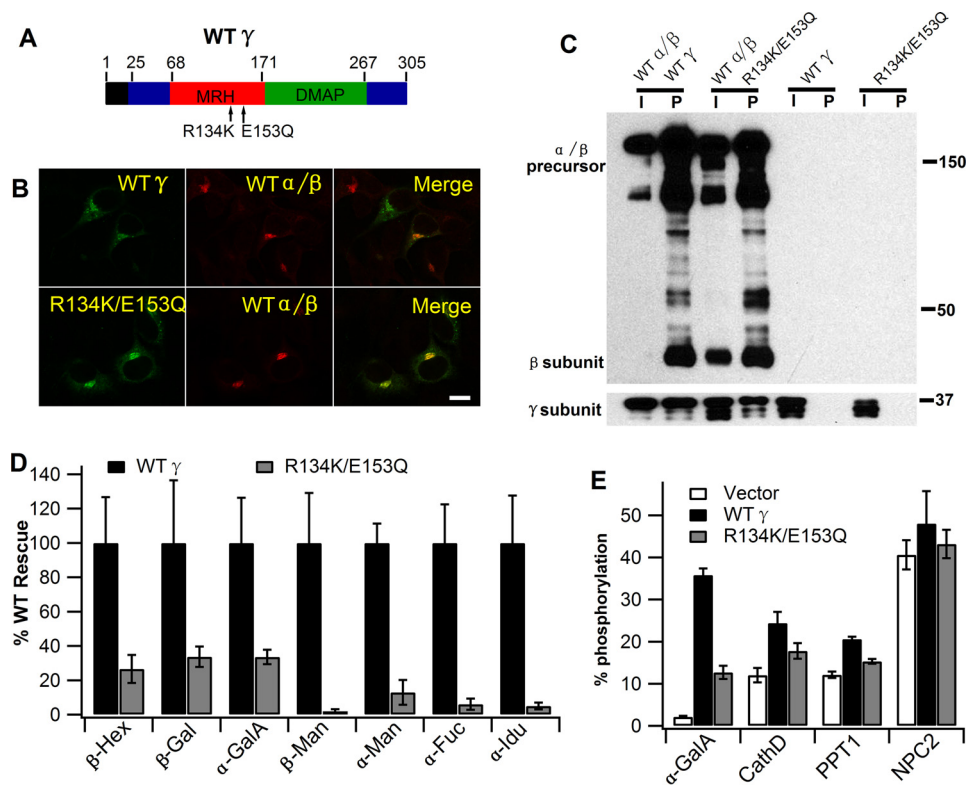


**FIGURE 9. Effect of mutating two critical residues in the  $\gamma$ MRH domain on lysosomal enzyme phosphorylation.** *A*, schematic showing the domain boundaries of the  $\gamma$  subunit and the position of the MRH mutations. *B*, confocal immunofluorescence images of *GNPTG*<sup>-/-</sup> cells co-transfected with WT  $\alpha/\beta$  and either WT  $\gamma$  or the R134K/E153Q MRH mutant. Scale bar, 10  $\mu$ m. *C*, lysates of HEK 293 cells expressing WT  $\alpha/\beta$  along with WT  $\gamma$  or the R134K/E153Q MRH mutant were incubated with Ni-NTA affinity beads to pull down the  $\alpha/\beta/\gamma$  complex. WT  $\gamma$  only and the R134K/E153Q MRH mutant only served as controls. The bound material was assayed for the content of  $\alpha/\beta$  and  $\gamma$  subunits by SDS-PAGE and Western blotting using anti-V5 antibody to detect  $\alpha/\beta$  and anti-FLAG antibody to detect  $\gamma$ . *I*, 3% of input; *P*, 25% of pellet fraction. *D*, lysates of *GNPTG*<sup>-/-</sup> HeLa cells expressing either WT  $\gamma$  or the R134K/E153Q MRH mutant were incubated with CI-MPR affinity beads, and the bound material was assayed for the content of the indicated acid glycosidases. Mean values obtained with the mutant are compared with WT  $\gamma$ , which is set to 100%  $\pm$  S.D. ( $n = 2-4$ ). *E*, *GNPTG*<sup>-/-</sup> cells were co-transfected with WT  $\gamma$  or the R134K/E153Q mutant, along with the indicated lysosomal protein encoding plasmids. Following [<sup>3</sup>H]mannose labeling, the degree of *N*-glycan phosphorylation of the lysosomal proteins was determined. The percentage oligosaccharide phosphorylation  $\pm$  S.D. for each enzyme with either empty vector, WT  $\gamma$ , or the MRH mutant are shown ( $n = 2-4$ ).

reposition the glycans sufficiently to allow successful phosphorylation (9). The findings presented here are fully consistent with this proposal. The binding of the  $\gamma$ DMAP interaction domain to the protein portion of the acceptor could aid in this process.

Taken together, these findings provide strong support for the hypothesis that mammalian GlcNAc-1-phosphotransferase evolved from an ancestral sugar-P-transferase gene that acquired the Notch repeat modules and the DMAP interaction domains along with a binding site for the  $\gamma$  subunit to meet the requirement to selectively recognize the 60 or so lysosomal proteins. These lysosomal proteins catalyze many different reactions and have a great variety of structures to perform these functions. Taking this into account, it is understandable that these 60 different proteins do not appear to share an identical conformation-dependent protein docking site for GlcNAc-1-phosphotransferase nor an *N*-linked glycan located a standard distance from the docking site. This speaks to the necessity to have flexibility in the function of GlcNAc-1-phosphotransferase. The involvement of two Notch repeat modules and the DMAP interaction domain of the  $\alpha$  subunit along with a second DMAP interaction domain and the MRH domain of the  $\gamma$  subunit would serve to provide the flexibility needed for binding the various lysosomal proteins and positioning their *N*-linked glycans so that they are accessible to the catalytic elements of the transferase.

**Author Contributions**—E. v. M., W. S. L., L. L., Y. Q., B. D., and S. K. designed the experiments; E. v. M., W. S. L., L. L., Y. Q., and B. D. performed and analyzed the experiments; E. v. M., W. S. L., L. L., B. D., and S. K. wrote the manuscript.

### References

- Kornfeld, S. (1986) Trafficking of lysosomal enzymes in normal and disease states. *J. Clin. Invest.* **77**, 1–6
- Reitman, M. L., and Kornfeld, S. (1981) Lysosomal enzyme targeting. *N*-Acetylglucosaminylphosphotransferase selectively phosphorylates native lysosomal enzymes. *J. Biol. Chem.* **256**, 11977–11980
- Varki, A., and Kornfeld, S. (1980) Identification of a rat liver  $\alpha$ -*N*-acetylglucosaminyl phosphodiesterase capable of removing “blocking”  $\alpha$ -*N*-acetylglucosamine residues from phosphorylated high mannose oligosaccharides of lysosomal enzymes. *J. Biol. Chem.* **255**, 8398–8401
- Bao, M., Booth, J. L., Elmendorf, B. J., and Canfield, W. M. (1996) Bovine UDP-*N*-acetylglucosamine:lysosomal-enzyme *N*-acetylglucosamine-1-phosphotransferase. I. Purification and subunit structure. *J. Biol. Chem.* **271**, 31437–31445
- Kudo, M., Bao, M., D’Souza, A., Ying, F., Pan, H., Roe, B. A., and Canfield, W. M. (2005) The  $\alpha$ - and  $\beta$ -subunits of the human UDP-*N*-acetylglucosamine:lysosomal enzyme *N*-acetylglucosamine-1-phosphotransferase [corrected] are encoded by a single cDNA. *J. Biol. Chem.* **280**, 36141–36149
- Raas-Rothschild, A., Cormier-Daire, V., Bao, M., Genin, E., Salomon, R., Brewer, K., Zeigler, M., Mandel, H., Toth, S., Roe, B., Munnich, A., and Canfield, W. M. (2000) Molecular basis of variant pseudo-hurler polydys-

- trophy (mucopolipidosis IIIC). *J. Clin. Invest.* **105**, 673–681
7. Tiede, S., Storch, S., Lübke, T., Henrissat, B., Bargal, R., Raas-Rothschild, A., and Braulke, T. (2005) Mucopolipidosis II is caused by mutations in GNPTA encoding the  $\alpha/\beta$  GlcNAc-1-phosphotransferase. *Nat. Med.* **11**, 1109–1112
  8. Kudo, M., and Canfield, W. M. (2006) Structural requirements for efficient processing and activation of recombinant human UDP-*N*-acetylglucosamine:lysosomal-enzyme-*N*-acetylglucosamine-1-phosphotransferase. *J. Biol. Chem.* **281**, 11761–11768
  9. Qian, Y., Lee, I., Lee, W. S., Qian, M., Kudo, M., Canfield, W. M., Lobel, P., and Kornfeld, S. (2010) Functions of the  $\alpha$ ,  $\beta$ , and  $\gamma$  subunits of UDP-GlcNAc:lysosomal enzyme *N*-acetylglucosamine-1-phosphotransferase. *J. Biol. Chem.* **285**, 3360–3370
  10. Qian, Y., van Meel, E., Flanagan-Steet, H., Yox, A., Steet, R., and Kornfeld, S. (2015) Analysis of mucopolipidosis II/III GNPTAB missense mutations identifies domains of UDP-GlcNAc:lysosomal enzyme GlcNAc-1-phosphotransferase involved in catalytic function and lysosomal enzyme recognition. *J. Biol. Chem.* **290**, 3045–3056
  11. Sperisen, P., Schmid, C. D., Bucher, P., and Zilian, O. (2005) Stealth proteins: *in silico* identification of a novel protein family rendering bacterial pathogens invisible to host immune defense. *PLoS Comput. Biol.* **1**, e63
  12. Rountree, M. R., Bachman, K. E., and Baylin, S. B. (2000) DNMT1 binds HDAC2 and a new co-repressor, DMAP1, to form a complex at replication foci. *Nat. Genet.* **25**, 269–277
  13. Qian, Y., Flanagan-Steet, H., van Meel, E., Steet, R., and Kornfeld, S. A. (2013) The DMAP interaction domain of UDP-GlcNAc:lysosomal enzyme *N*-acetylglucosamine-1-phosphotransferase is a substrate recognition module. *Proc. Natl. Acad. Sci. U.S.A.* **110**, 10246–10251
  14. Munro, S. (2001) The MRH domain suggests a shared ancestry for the mannose 6-phosphate receptors and other *N*-glycan-recognising proteins. *Curr. Biol.* **11**, R499–501
  15. Castonguay, A. C., Olson, L. J., and Dahms, N. M. (2011) Mannose 6-phosphate receptor homology (MRH) domain-containing lectins in the secretory pathway. *Biochim. Biophys. Acta* **1810**, 815–826
  16. Hosokawa, N., Kamiya, N., Kamiya, D., Kato, K., and Nagata, K. (2009) Human OS-9, a lectin required for glycoprotein endoplasmic reticulum-associated degradation, recognizes mannose-trimmed *N*-glycans. *J. Biol. Chem.* **284**, 17061–17068
  17. Hu, D., Kamiya, Y., Totani, K., Kamiya, D., Kawasaki, N., Yamaguchi, D., Matsuo, I., Matsumoto, N., Ito, Y., Kato, K., and Yamamoto, K. (2009) Sugar-binding activity of the MRH domain in the ER  $\alpha$ -glucosidase II  $\beta$  subunit is important for efficient glucose trimming. *Glycobiology* **19**, 1127–1135
  18. De Pace, R., Velho, R. V., Encarnação, M., Marschner, K., Braulke, T., and Pohl, S. (2015) Subunit interactions of the disease-related hexameric GlcNAc-1-phosphotransferase complex. *Hum. Mol. Genet.* **24**, 6826–6835
  19. Valenzano, K. J., Remmler, J., and Lobel, P. (1995) Soluble insulin-like growth factor II/mannose 6-phosphate receptor carries multiple high molecular weight forms of insulin-like growth factor II in fetal bovine serum. *J. Biol. Chem.* **270**, 16441–16448
  20. Cunningham, M., and Tang, J. (1976) Purification and properties of cathepsin D from porcine spleen. *J. Biol. Chem.* **251**, 4528–4536
  21. Canduri, F., Ward, R. J., de Azevedo Júnior, W. F., Gomes, R. A., and Arni, R. K. (1998) Purification and partial characterization of cathepsin D from porcine (*Sus scrofa*) liver using affinity chromatography. *Biochem. Mol. Biol. Int.* **45**, 797–803
  22. Dustin, M. L., Baranski, T. J., Sampath, D., and Kornfeld, S. (1995) A novel mutagenesis strategy identifies distantly spaced amino acid sequences that are required for the phosphorylation of both the oligosaccharides of procathepsin D by *N*-acetylglucosamine 1-phosphotransferase. *J. Biol. Chem.* **270**, 170–179
  23. Tong, P. Y., Gregory, W., and Kornfeld, S. (1989) Ligand interactions of the cation-independent mannose 6-phosphate receptor. The stoichiometry of mannose 6-phosphate binding. *J. Biol. Chem.* **264**, 7962–7969
  24. Marschner, K., Kollmann, K., Schweizer, M., Braulke, T., and Pohl, S. (2011) A key enzyme in the biogenesis of lysosomes is a protease that regulates cholesterol metabolism. *Science* **333**, 87–90
  25. Hancock, M. K., Haskins, D. J., Sun, G., and Dahms, N. M. (2002) Identification of residues essential for carbohydrate recognition by the insulin-like growth factor II/mannose 6-phosphate receptor. *J. Biol. Chem.* **277**, 11255–11264
  26. Gordon, W. R., Vardar-Ulu, D., Histen, G., Sanchez-Irizarry, C., Aster, J. C., and Blacklow, S. C. (2007) Structural basis for autoinhibition of Notch. *Nat. Struct. Mol. Biol.* **14**, 295–300
  27. Boldt, H. B., Kjaer-Sorensen, K., Overgaard, M. T., Weyer, K., Poulsen, C. B., Sottrup-Jensen, L., Conover, C. A., Giudice, L. C., and Oxvig, C. (2004) The Lin12-notch repeats of pregnancy-associated plasma protein-A bind calcium and determine its proteolytic specificity. *J. Biol. Chem.* **279**, 38525–38531
  28. Weyer, K., Boldt, H. B., Poulsen, C. B., Kjaer-Sorensen, K., Gyrupe, C., and Oxvig, C. (2007) A substrate specificity-determining unit of three Lin12-Notch repeat modules is formed in trans within the pappalysin-1 dimer and requires a sequence stretch C-terminal to the third module. *J. Biol. Chem.* **282**, 10988–10999
  29. Goldberg, D. E., and Kornfeld, S. (1981) The phosphorylation of  $\beta$ -glucuronidase oligosaccharides in mouse P388D1 cells. *J. Biol. Chem.* **256**, 13060–13067
  30. Sonderfeld-Fresko, S., and Proia, R. L. (1989) Analysis of the glycosylation and phosphorylation of the lysosomal enzyme,  $\beta$ -hexosaminidase B, by site-directed mutagenesis. *J. Biol. Chem.* **264**, 7692–7697
  31. Weitz, G., and Proia, R. L. (1992) Analysis of the glycosylation and phosphorylation of the  $\alpha$ -subunit of the lysosomal enzyme,  $\beta$ -hexosaminidase A, by site-directed mutagenesis. *J. Biol. Chem.* **267**, 10039–10044
  32. Gieselmann, V., Schmidt, B., and von Figura, K. (1992) *In vitro* mutagenesis of potential *N*-glycosylation sites of arylsulfatase A. Effects on glycosylation, phosphorylation, and intracellular sorting. *J. Biol. Chem.* **267**, 13262–13266
  33. Shipley, J. M., Grubb, J. H., and Sly, W. S. (1993) The role of glycosylation and phosphorylation in the expression of active human  $\beta$ -glucuronidase. *J. Biol. Chem.* **268**, 12193–12198
  34. Cantor, A. B., and Kornfeld, S. (1992) Phosphorylation of Asn-linked oligosaccharides located at novel sites on the lysosomal enzyme cathepsin D. *J. Biol. Chem.* **267**, 23357–23363
  35. Warner, J. B., Thalhauser, C., Tao, K., and Sahagian, G. G. (2002) Role of *N*-linked oligosaccharide flexibility in mannose phosphorylation of lysosomal enzyme cathepsin L. *J. Biol. Chem.* **277**, 41897–41905